Journal of Photochemistry and Photobiology A: Chemistry 205 (2009) 93–97

Contents lists available at ScienceDirect

Journal of Photochemistry and Photobiology A: Chemistry

journal homepage: www.elsevier.com/locate/jphotochem

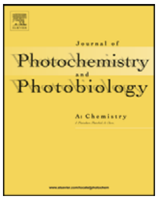

# Nitrogen-doped and nitrogen–fluorine-codoped titanium dioxide. Nature and concentration of the photoactive species and their role in determining the photocatalytic activity under visible light

S. Livraghi[a], K. Elghniji[b], A.M. Czoska[a], M.C. Paganini[a], E. Giamello[a,*], M. Ksibi[b]

[a] Dipartimento di Chimica I.F.M. and NIS, Università degli Studi di Torino, Via P. Giuria, 7 10125 Torino, Italy
[b] Laboratoire Eau, Energie et Environnement (LR3E), Ecole Nationale d'Ingénieurs de Sfax, BP W 3038, Sfax, Tunisia

ARTICLE INFO

*Article history:*
Received 2 March 2009
Received in revised form 2 April 2009
Accepted 20 April 2009
Available online 3 May 2009

*Keywords:*
Nitrogen-doped titanium dioxide
Photocatalytic activity under visible light
Optical absorption
EPR spectroscopy

ABSTRACT

Two series of N-doped and N, F-codoped titanium dioxide samples having different loading of impurity were prepared using sol–gel synthesis and successive calcinations in air. Ammonium chloride and ammonium fluoride were used as source of dopants in the two cases. In all cases the insertion of nitrogen is observed which determines the optical absorption in the visible of the materials and their photocatalytic activity under solar light. This was investigated following the decomposition of methylene blue in aqueous phase. Two photoactive species (describable in terms of $NO^{2-}$ and $NO^{3-}$ bulk species) determine the optical absorption in the visible range. The former one (paramagnetic) is detectable by Electron Paramagnetic Resonance (EPR) and its intensity in all samples is roughly proportional to the optical absorption at 440 nm. The photocatalytic activity under solar light directly depends on the concentration of the nitrogen photoactive species in the solid till a saturation limit, which in turn, depends on the concentration of ammonium ions in the starting solution and on the heating rate during calcinations. The use of ammonium fluoride in the synthesis promotes N insertion and increments the photocatalytic activity due to the fact that, differently from $Cl^-$ ions, $F^-$ ions substitutes oxygen in the solid lattice giving rise to electronic effects which favour N photoactive species incorporation in the solid.

## 1. Introduction

A large number of investigations have been undertaken in recent years concerning the doping of titanium dioxide by non-metal p-block elements, and in particular by nitrogen, in order to reduce the absorption threshold of the oxide and to make it photosensitive to visible light [1–4]. Many observations have shown that nitrogen-doped titanium dioxide, N–$TiO_2$, exhibits optical properties different from those of the bare oxide owing to the onset of absorption in the visible region of the spectrum. This is accompanied by the evidence of photocatalytic activity in various reactions for pollutants abatement performed under visible light irradiation [5–16].

This activity is higher than that observed, under the same type of irradiation, for the bare oxide and further increases if $TiO_2$ is doped with nitrogen and fluorine atoms together (N, F-$TiO_2$) [17]. The reason of the peculiar optical absorption and of the enhanced catalytic activity for both singly doped and codoped systems is still under discussion [18,19] in particular as far as the nature of the photoactive nitrogen species and the electronic structure of the doped solid are concerned. Our group has recently published a series of papers on the electronic structure of singly doped (N-$TiO_2$, F-$TiO_2$) [20–24] and codoped (N, F-$TiO_2$) [25] solids. The solids were prepared with a classic sol–gel procedure using aqueous solutions containing $NH_4^+$ and/or $F^-$ ions (nitrogen and fluorine source respectively) to hydrolyze the titanium alkoxide. Calcinations in air to obtain the final oxidic material were eventually performed. Our analysis was based on the combined use of Electron Paramagnetic Resonance (EPR) spectroscopy and state of the art DFT theoretical calculations [20,23–25]. Due to the paramagnetic nature of some of the extrinsic defects introduced by doping into the oxide matrix, we could couple the EPR spectra of the defects with theoretical modeling. In this way it has been basically shown that:

(a) In N-$TiO_2$ a bulk nitrogen paramagnetic species, initially labeled $N_b^{\bullet}$, forms which lies some tenth of eV over the limit of the valence band and is selectively excited by visible light with $\lambda = 440$ nm, this wavelength roughly corresponding to the maximum of the optical absorption in the visible [25]. This species can be seen as an interstitial N atom stuck to a lattice $O^{2-}$ ion forming so far a π system also describable as $NO^{2-}$ and exists in equilibrium with a diamagnetic companion bearing

---

* Corresponding author. Tel.: +39 011 6707574.
*E-mail address:* elio.giamello@unito.it (E. Giamello).

1010-6030/$ – see front matter © 2009 Elsevier B.V. All rights reserved.
doi:10.1016/j.jphotochem.2009.04.010

one electron more ($N_b^-$, $NO^{3-}$). Both species are responsible of the optical absorption in the visible (yellow color) of the solids.

(b) Fluorine enters in the lattice substituting oxygen. The extra electron associated to the heteroatom is localized by $Ti^{4+}$ ions forming shallow electron states ($Ti^{3+}$) whose energy lies in the band gap very close to the conduction band limit [23].

(c) The codoped system is stabilized by electron transfer from the upper lying states ($Ti^{3+}$) to the lower ones, $N_b^\bullet$, which occurs spontaneously increasing the concentration of $N_b^-$ and decreasing that of $Ti^{3+}$.

The present investigation on both N-doped and N–F-codoped systems moved from the idea of analyzing the preparation of the materials in order to find out correlations (if any) linking the concentration of the doping agent present in solution during preparation, the doping degree of the solid and the photocatalytic activity of the systems. The degradation of Methylene Blue (MB) in visible light was selected for the photocatalysis test. The two series of materials were prepared using $NH_4Cl$ and $NH_4F$ as dopant source for N-$TiO_2$ and N, F-$TiO_2$. It is known in fact that $Cl^-$ is not capable to dope titania while $F^-$ has a certain propensity to substitute $O^{2-}$ in the lattice [23]. It is worth noting that in the second case the two doping elements are present in equivalent concentration in the starting solution. However, only a relatively small fraction of the dopants present in the solution enters in the solid composition whose chemical analysis, by the way, is hampered by the simultaneous presence of various by-products of calcinations and unreacted $NH_4^+$ ions [26,27]. For these reasons we have adopted the optical absorption at 440 nm (corresponding to the maximum visible light absorption of doped samples) as a rough but significant measure of the concentration of photoactive nitrogen species into the various materials. The validation of this choice will be discussed in the following in present article. The correlation between the amount of dopants incorporated in the oxide and some parameters of the preparation procedure (in particular the rate of temperature increase during calcination) have also been investigated.

## 2. Experimental

Two series of singly doped (N-$TiO_2$) and of codoped (N, F-$TiO_2$) were prepared both composed of five members. Each member was prepared using in the starting solution a concentration of the dopant source, ($NH_4Cl$ and $NH_4F$ respectively) in order to achieve a nominal molar doping of the dopant elements respectively of 1%, 5%, 10%, 20%, and 30%. In Table 1 the labels employed in this work to identify the different samples and the corresponding surface area obtained by B.E.T. measurements are reported. The presence of both N and F centres in the codoped system has been previously demonstrated [24].

**Table 1**
Abbreviation adopted for the samples of the present work and the corresponding surface areas.

| Samples abbreviation | Fraction (%) of dopant in the starting solution | B.E.T. ($m^2/g$) |
|---|---|---|
| Pure | 0 | 106 |
| N-$TiO_2$ | | |
| N1 | 1 | 90 |
| N5 | 5 | 65 |
| N10 | 10 | 70 |
| N20 | 20 | 70 |
| N30 | 30 | 60 |
| N, F-$TiO_2$ | | |
| NF1 | 1 | 102 |
| NF5 | 5 | 32 |
| NF10 | 10 | 31 |
| NF20 | 20 | 32 |
| NF30 | 30 | 34 |

The two series of samples (1–30%) were prepared via hydrolysis of titanium (IV) isopropoxide with $NH_4Cl$ or $NH_4F$ aqueous solutions (0.1, 0.3, 0.6, 1.3 and 1.9 mol/l, respectively), with a molar ratio of $Ti/H_2O = 0.1$. The product was left ageing for 15 h at room temperature and subsequently dried at 70 °C until a completed drying. The dried material was eventually calcined in air at 770 K for 1 h using heating rate of 20 °C/min. In the case of codoped materials a second heating rate of 5 °C/min was used also in order to evaluate the effect of this preparation parameter on the final product.

As a reference material, bare $TiO_2$ was prepared using the same procedure avoiding addition of ammonia salts during hydrolysis.

Structural features of the prepared materials have been determined by X-ray diffraction (XRD) on a Philips 1830 XRD spectrometer using a K$\alpha$ (Co) source. UV–Vis. diffuse reflectance (DR UV–Vis.) spectra were recorded by a Varian Cary 5/UV–Vis.-N.I.R. spectrometer using a Cary win-UV scan software to follow the visible absorption enhancement due to nitrogen doping. Surface area was measured by a fully automated surface area analyzer (ASAP 2020 Accelerated Surface Area and Porosimetry, Micromeritics, USA).

Electron Paramagnetic Resonance (EPR) spectra were run using a X-band CW-EPR Bruker EMX spectrometer equipped with a cylindrical cavity operating at 100 kHz field modulation. The measurements were carried out in cells that can be connected to a conventional high-vacuum apparatus (residual pressure $<10^{-6}$ kPa). The EPR spectra intensity has been obtained by double integration of the signals recorded for each samples, using in all test the same amount of sample.

Samples photoactivity was tested using the Methylene Blue (MB) photodegradation reaction in liquid phase [28,29] which was carried out as follows: first the catalysts (0.01 g) was suspended in the dye solution (10 ml, 5 mg/l) for 30 min in the dark to establish the adsorption–desorption equilibrium of MB, then irradiated in a solar box (dr.Hoenle SOL2, 400 W). The residual MB concentration as a function of time was monitored using a spectrophotometric method on a Cary 300 Bio UV–Visible Spectrophotometer. For each measurements dye solution was separated from the catalyst filtering the suspension with teknocroma nylon syringe filter ($\phi = 13$ mm, pore diameter 0.45 $\mu$m).

## 3. Results and discussion

### 3.1. Optical absorption in the visible range and XRD analysis

All samples prepared for the present work were analyzed by X-ray diffraction (XRD). The results are similar to those reported in previous papers [26]. The codoped N, F-$TiO_2$ samples have a higher crystallinity than the corresponding N-$TiO_2$ ones. All samples show anatase structure except for the samples N5, N1 and NF1 which show a small, but however negligible, fraction of brookite polymorph.

Fig. 3A shows the DR-UV–Vis. spectra of the series of samples from NF1 to NF30. The visible absorption intensity (a broad band with maximum at around 440) growths from NF1 to NF30 in parallel with the color of the solids progressively evolving from a very pale yellow to a more vivid yellow. As briefly mentioned in the introduction a quantitative analysis limited to those species responsible for visible light absorption is hard to perform as nitrogen is present in the solid under various forms including, beside bulk $NO^{2-}$ and $NO^{3-}$ species, unreacted ammonium ions, oxidation products like NO, cyanide groups, etc. [26].

The most convenient way to have a rough measure of the effectiveness of doping has to be based on the intensity of the absorption

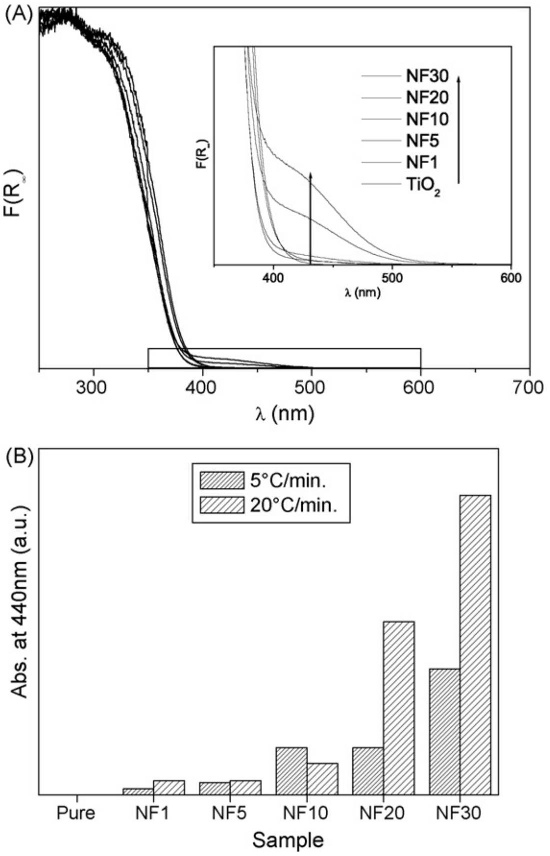

**Fig. 1.** (A) DR-UV–Vis. spectra of N, F-codoped $TiO_2$ samples. (B) Maximum optical absorption (440 nm) for the same materials prepared with two different heating rates (5 °C/min, 20 °C/min).

in correspondence of its maximum. This criterion will thus be adopted in the following of the present work.

The concentration of the solution used in the preparation is, as expected and as shown in Fig. 1A, a parameter influencing the final concentration of doping centres. A second parameter is the rate of temperature increase during calcinations. This is also shown in Fig. 1B where the absorption maxima at 440 nm are reported for all N–F sample prepared using rates of temperature increase of 5 K/min and 20 K/min, respectively. It is easily observed that the effect of the heating rate is negligible at low N loading but becomes important at higher loading (NF20, NF30). The incorporation of photoactive species is favoured by a higher rate of temperature increase during calcinations. Fig. 2 reports the DR-UV–Vis. spectra of the series of samples from N1 to N30 using 20 K/min as a heating rate during calcination. The optical absorption in the visible region is lower than in the case of codoped materials (*vide infra*).

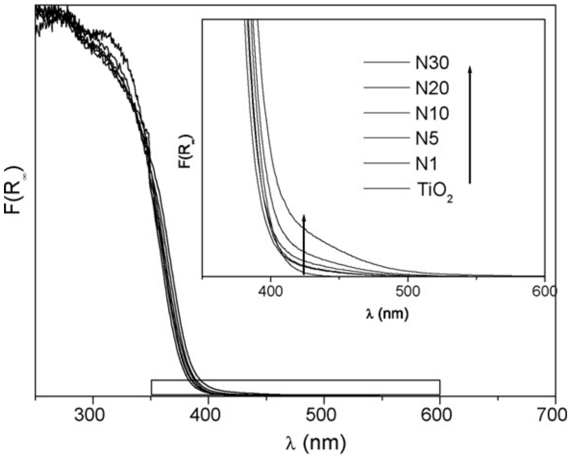

**Fig. 2.** DR-UV–Vis. spectra of N-doped $TiO_2$ samples.

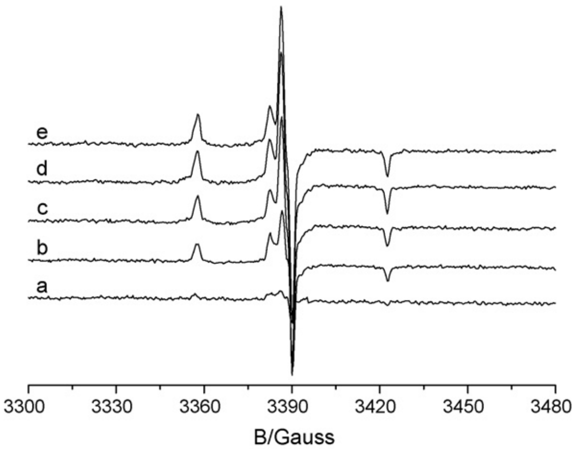

**Fig. 3.** EPR spectra of $N_b^{\bullet}$ species in the series of N-$TiO_2$ from N1 (a) to N30 (e).

### 3.2. Optical absorption and paramagnetic species

As reported in the introduction, N-doped $TiO_2$ is characterized by the presence of a paramagnetic species ($NO^{2-}$ or $N_b^{\bullet}$) whose EPR spectrum has been discussed in previous works [25,30]. The identification of this paramagnetic species as the centre (or one of the centres) directly responsible of visible light absorption was proposed on the basis of irradiation experiments showing that the EPR spectral intensity of the species itself varies irradiating the sample with light having wavelength corresponding to the maximum of the optical absorption [25]. It is now possible to confirm this finding, which is of fundamental importance to understand the nature of N-doped $TiO_2$, on the basis of a comparison of materials having different dopant concentration. Fig. 3 reports the series of EPR spectra recorded for the whole series of N-$TiO_2$ samples calcined at 20 K/min. The powder spectrum is characterized by a signal having a triplet of lines due to the hyperfine interaction of the unpaired electron with the $^{14}N$ nucleus (nuclear spin I = 1) and has been thoroughly discussed elsewhere [25]. The intensities of these spectra (obtained by double integration of the signals) are compared with absorption at 440 nm of the optical spectra in Fig. 4.

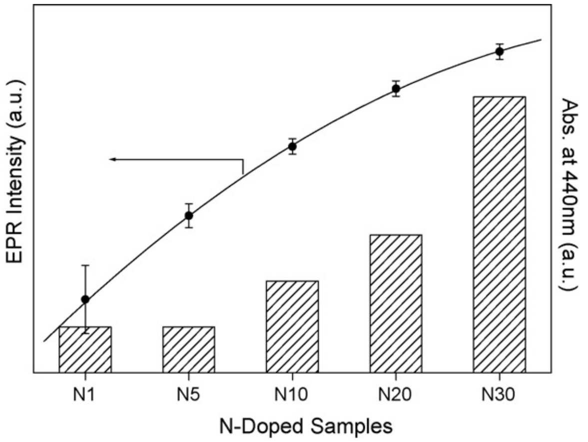

**Fig. 4.** EPR intensity ($N_b^{\bullet}$) and optical absorption at 440 nm for N-$TiO_2$ samples.

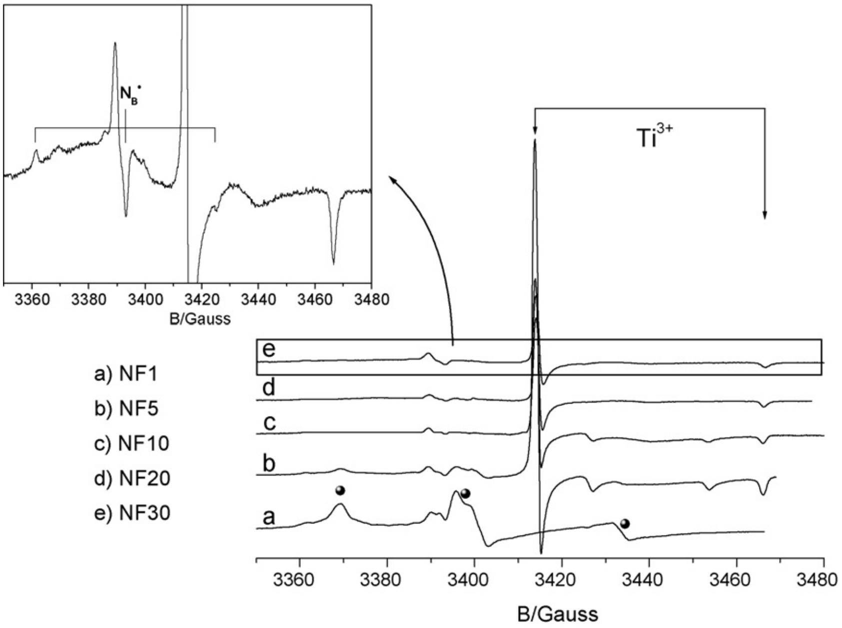

**Fig. 5.** EPR spectra of N, F-$TiO_2$ samples recorded at 77 K and 1 mW microwave power. (● ) Indicates the main features of the EPR signal of molecular NO. Arrows indicate the $Ti^{3+}$ signal. The inset shows the magnification of the spectrum of sample NF30 where the $N_b^•$ species can be easily recognised.

For the sake of clarity is correct to recall that while EPR intensity is related to the only $N_b^•$ paramagnetic species, the optical absorption is based on the contribute of both $N_b^•$ and diamagnetic counterpart ($N_b^-$) [25]. The proportionality of EPR and optical absorption intensities suggests that the ratio between $N_b^•$ and $N_b^-$ is roughly constant in the solids and that both species are responsible of the visible light absorption in N containing titania. The similar growing trend of the two parameters (Fig. 4) is a further convincing prove of the fact that $N_b^•$ is responsible, together with its diamagnetic counterpart $N_b^-$ of the visible light absorption in N-doped titania. The same correlation shown in Fig. 4 for N-$TiO_2$ has not been performed for the codoped N, F-$TiO_2$ materials as, in that case, the overlap of the $N_b^•$ EPR features with those of the $Ti^{3+}$ paramagnetic centers and the interplay between the two centers [24] prevents a correct quantitative evaluation (Fig. 5).

Fig. 5 reports the EPR spectra of the N, F-codoped samples recorded at low temperature. In this series of samples three different signals can be observed by EPR which are respectively: (i) the $N_b^•$ species, (ii) the signal due to molecular NO trapped in the bulk of the solid and (iii) the $Ti^{3+}$ signal consequence of fluorine doping. At high concentration of dopants the trapped NO amount decreases and the $Ti^{3+}$ species shows up. Because of the simultaneously presence of this complex set of overlapping signals an accurate evaluation of the $N_b^•$ signal intensity cannot be performed as in the case of N-$TiO_2$ systems.

### 3.3. Role of fluorine in codoped materials

Fluorine easily enters in the $TiO_2$ lattice in substitutional positions taking the place of oxygen ions whereas chlorine does not [23]. Fig. 6A compares the optical absorption at 440 nm for the two series of samples obtained via ammonium chloride and ammonium fluoride, respectively. There are not remarkable differences for low concentrations materials but the differences are dramatic for higher concentration ones (20%, 30%).

In these high loading materials the main effect of the presence of F, as inferred in a previous work [24], favours the introduction of nitrogen active species since the extra electron introduced by F in the system can be transferred to the low energy orbitals of $N_b^•$ (which reduces to $N_b^-$) with a consistent energy gain, in electronic terms, for the whole system. The presence of fluorine in substitutional positions of the oxide lattice entails therefore a synergistic effect leading to an improved capability of the solid to host N dopants. This effect is not visible for materials from 1% to 10%

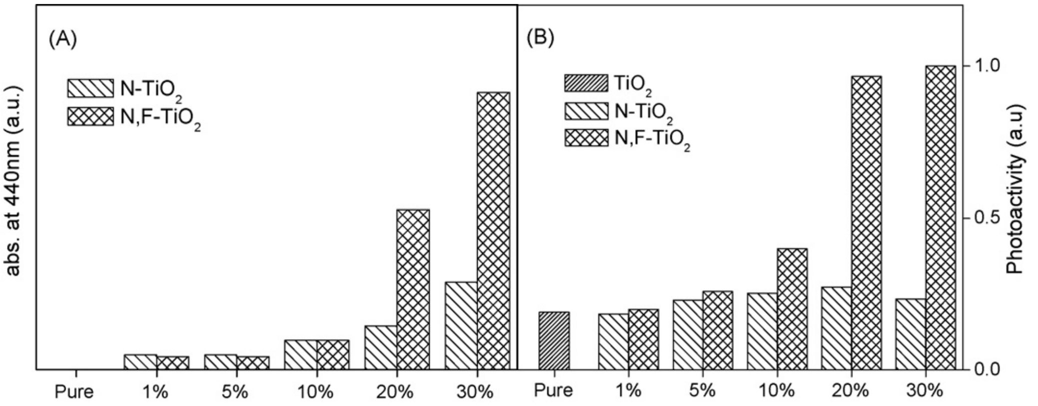

**Fig. 6.** (A) Comparison of optical absorption at 440 nm for N-$TiO_2$ and N, F-$TiO_2$ materials. (B) Comparison of photocatalytic activity for MB degradation under solar light for N-$TiO_2$ and N, F-$TiO_2$ materials. The values (a.u.) are normalized on the specific surface area.

probably because of low efficiency, at low concentrations, of the process of $F^-$ incorporation in the bulk of oxide. A further possible contribution of fluorine to the catalytic activity is related to $F^-$ ions stabilized at the surface during the preparation of the materials in $NH_4F$ solutions. Each surface $F^-$ ion substitutes an isoelectronic $OH^-$ group with no alteration of the charge balance. This is the reason why surface fluorinated $TiO_2$ is EPR silent [23]. However it was reported that surface fluorination has some influence in promoting the photocatalytic activity under ultraviolet irradiation [31,32]. A role of this second type of fluoride ions in the photocatalytic activity of the materials here described cannot be discarded even though it is reasonably lower than that of the bulk ions.

Fig. 6 reports the photocatalytic activity in MB degradation performed in a solar box apparatus simulating the solar light (B) in parallel with the visible light absorption of the two series of doped samples (A). The photocatalytic activity is reported in terms of MB degradation after 30 min of irradiation. All samples display some activity including $TiO_2$ due to small fraction of UV light present in the solar radiation. The trend of Fig. 6B is parallel to that of Fig. 6A, and comparison of the two figures can be resumed as follows:

(i) The photocatalytic activity of N-$TiO_2$ and N, F-$TiO_2$ is similar from 1% to 10% nominal doping even though the codoped samples are always slightly more active.
(ii) The behaviour is very different at high loading as NF20 and NF30 materials have an activity remarkably higher than that of N20 and N30.
(iii) The photocatalytic activity of NF30 is only slightly higher than that of NF20 indicating the onset, beyond a certain limit, of a sort of saturation.

The reason of this apparent saturation of the system has to be searched, as already reported in the literature [5,33–42] in the formation at high doping level of a progressively increasing number of charge recombination centres. The most striking fact deduced from Fig. 6 remains the strict parallel between optical absorption and catalytic activity. This result has two basic consequences: (a) the photocatalytic activity in visible light of N containing $TiO_2$ is related (till a saturation limit) to the concentration of N photoactive species in $TiO_2$. (b) This concentration remarkably growths with the assistance of $F^-$ ions introduced in the solid whose role is of favouring the N insertion due to the already described synergic effect.

## 4. Conclusions

In this work we have successfully synthesized N-doped $TiO_2$ and N- and F-codoped $TiO_2$ by hydrolysis of Ti-alkoxide in presence of $NH_4Cl$ and $NH_4F$. Nitrogen doping leads to yellow materials active in photocatalytic reaction under visible light irradiation.

The concentration of nitrogen photoactive species in the solid is proportional to the photocatalytic activity till a saturation limit and depends on:

(a) The concentration of $NH_4^+$ ions in the solution employed for the synthesis.
(b) The heating rate during calcinations.
(c) The concentration of $F^-$ ions which promotes N insertion.

The reported results confirm the potential of doped $TiO_2$ materials in the field of solar energy conversion and outline the role of fluorine in promoting the insertion of nitrogen photoactive species in titania.

## References

[1] R. Asahi, T. Morikawa, T. Ohwaki, K. Aoki, Y. Taga, Science 293 (2001) 269–271.
[2] T.L. Thompson, J.T. Yates Jr., Chem. Rev. 106 (2006) 4428–4453.
[3] X. Chen, S.S. Mao, Chem. Rev. 107 (2007) 2891–2959.
[4] C. Di Valentin, U. Diebold, A. Selloni (Guest Editors). Special Issue in Chemical Physics: Doping and functionalization of photo-active semiconducting oxides 339 (2007) 1–192.
[5] H. Irie, Y. Watanabe, K. Hashimoto, J. Phys. Chem. B 107 (2003) 5483–5486.
[6] S. Sakthivel, M. Janczarek, H. Kisch, J. Phys. Chem. B 108 (2004) 19384–19387.
[7] M. Miyauchi, A. Ikezawa, H. Tobimatsu, H. Irie, K. Hashimoto, Phys. Chem. Chem. Phys. 6 (2004) 865–870.
[8] O. Diwald, T.L. Thompson, T. Zubkov, E.G. Goralski, S.D. Walck, J.T. Yates, J. Phys. Chem. B 108 (2004) 6004–6008.
[9] M. Mrowetz, W. Balcerski, A.J. Colussi, M.R. Hoffmann, J. Phys. Chem. B 108 (2004) 17269–17273.
[10] J.L. Gole, J.D. Stout, C. Burda, Y. Lou, X. Chen, J. Phys. Chem. B 108 (2004) 1230–1240.
[11] S. Sato, R. Nakamura, S. Abe, Appl. Catal. B 284 (2005) 131–137.
[12] Z. Lin, A. Orlov, R.M. Lambert, M.C. Payne, J. Phys. Chem. B 109 (2005) 20948–20952.
[13] M. Sathish, B. Viswanathan, R.P. Viswanath, C.S. Gopinath, Chem. Mater. 17 (2005) 6349–6353.
[14] Y. Nosaka, M. Matsushita, J. Nasino, A.Y. Nosaka, Sci. Technol. Adv. Mater. 6 (2005) 143–148.
[15] M. Alvaro, E. Carbonell, V. Fornés, H. Garcia, ChemPhysChem 7 (2006) 200–205.
[16] Y. Irokawa, T. Morikawa, K. Aoki, S. Kosaka, T. Ohwaki, Y. Taga, Phys. Chem. Chem. Phys. 8 (2006) 1116–1121.
[17] D. Li, N. Ohashi, S. Hishita, T. Kolodiazhnyi, H. Haneda, J. Solid State Chem. 178 (2005) 3293–3302.
[18] A.V. Emeline, V.N. Kunznetsov, V.K. Rybchuk, N. Sermone, Int. J. Photoenergy 2008 (2008) 19, doi:10.1155/2008/258394, Article ID 258394.
[19] R. Asahi, T. Morikawa, Chem. Phys. 339 (2007) 57–63.
[20] C. Di Valentin, G. Pacchioni, A. Selloni, S. Livraghi, E. Giamello, J. Phys. Chem. B 109 (2005) 11414–11419.
[21] S. Livraghi, A.M. Czoska, M.C. Paganini, E. Giamello, J. Solid State Chem. 182 (2009) 160–164.
[22] C. Di Valentin, E. Finazzi, G. Pacchioni, A. Selloni, S. Livraghi, M.C. Paganini, E. Giamello, Chem. Phys. 339 (2007) 44–56.
[23] A.M. Czoska, S. Livraghi, M. Chiesa, E. Giamello, E. Finazzi, C. Di Valentin, G. Pacchioni, S. Agnoli, G. Granozzi, J. Phys. Chem. C 112 (2008) 8951–8956.
[24] C. Di Valentin, E. Finazzi, G. Pacchioni, A. Selloni, S. Livraghi, A.M. Czoska, M.C. Paganini, E. Giamello, Chem. Mater. 20 (2008) 3706–3714.
[25] S. Livraghi, M.C. Paganini, E. Giamello, A. Selloni, C. Di Valentin, G. Pacchioni, J. Am. Chem. Soc. 128 (2006) 15666–15671.
[26] S. Livraghi, M.R. Chierotti, E. Giamello, G. Magnacca, M.C. Paganini, G. Cappelletti, C.L. Bianchi, J. Phys. Chem. C 112 (2008) 17244–17252.
[27] R. Berenek, H.J. Kisch, Photochem. Photobiol. Sci. 7 (2008) 40–48.
[28] Q. Wang, C. Chen, D. Zhao, W. Ma, J. Zhao, Langmuir 24 (2008) 7338–7345.
[29] C. Burda, Y. Lou, X. Chen, A.C. Samia, S. Stout, J.L. Gole, Nanoletters 3 (2003) 1049–1051.
[30] S. Livraghi, A. Votta, M.C. Paganini, E. Giamello, Chem. Commun. 4 (2005) 498–500.
[31] C. Minero, G. Mariella, V. Maurino, E. Pelizzetti, Langmuir 16 (2000) 2632.
[32] C. Minero, G. Mariella, V. Maurino, D. Vione, E. Pelizzetti, Langmuir 16 (2000) 8964.
[33] S.Z. Chen, P.Y. Zhang, D.M. Zhuang, W.P. Zhu, Catal. Commun. 5 (2004) 677–680.
[34] Y. Nosaka, M. Matsushita, J. Nishino, A.Y. Nosaka, Sci. Technol. Adv. Mater. 6 (2005) 143–148.
[35] H. Li, J. Li, Y. Huo, J. Phys. Chem. B 110 (2006) 1559–1565.
[36] C. Belver, R. Bellod, S. Stewart, F. Requejo, M. Garcia, Appl. Catal. B: Environ. 65 (2006) 309–314.
[37] Y. Wang, C. Feng, Z. Jin, J. Zhang, J. Yang, S. Zhang, J. Mol. Catal. A: Chem. 160 (2006) 1–3.
[38] W. Belcerski, S.Y. Ryu, M.R. Hoffman, J. Phys. Chem. C 111 (2007) 15357–15362.
[39] E. Martinez - Ferro, Y. Sakatami, C. Boissière, D. Grosso, A. Fuertes, J. Fraxdes, C. Sanchez, Adv. Funct. Mater. 17 (2007) 3348–3354.
[40] R. Berenek, H. Kisch, Electrochem. Commun. 9 (2007) 761–766.
[41] C. Feng, Y. Wang, Z. Jin, J. Zhang, S. Zhang, Z. Wu, Z. Zhang, New J. Chem. 32 (2008) 1038–1047.
[42] T. Okumura, Y. Kinoshita, H. Uchiyama, H. Imai, Mater. Chem. Phys. 111 (2008) 486–490.